An exact band-structure method applied to the three-dimensional Mathieu problem

1990 J. Phys.: Condens. Matter 2 5689

(http://iopscience.iop.org/0953-8984/2/26/005)

J. Phys.: Condens. Matter **2** (1990) 5689–5702. Printed in the UK

An exact band-structure method applied to the three-dimensional Mathieu problem

I I Gegusin and L I Leontieva
Institute of Physics, Rostov State University, pr. Stachky 194, Rostov on Don 344104, USSR

Received 30 October 1989, in final form 26 February 1990

Abstract. A method assigned to solve exactly the Schrödinger equation with non-muffin-tin crystal potential is numerically tested. The approach is based on the Green function technique. It differs from the conventional multiple-scattering methods in that the wave field ψ_k is sought at some points within a cell rather than at the boundaries. The empty lattice and three-dimensional Mathieu problems are studied with the emphasis on convergence properties. Generally, the convergence is governed by three independent parameters, resulting as a consequence of the truncation of some infinite series, namely, the expansions of the Green function, potential and wavefunction ψ_k sought. It is numerically shown that, by increasing the three parameters mentioned, the calculated energy eigenvalues approach the exact ones.

1. Introduction

The eigenstates ψ_k of a one-electron crystal Hamiltonian are determined as finite solutions of the following boundary-value problem

$$\begin{aligned} &[-\nabla^2 + V(\boldsymbol{r}) - E]\psi_k(\boldsymbol{r}) = 0 \\ &V(\boldsymbol{r}+\boldsymbol{R}_n) = V(\boldsymbol{r}) \qquad \psi_k(\boldsymbol{r}+\boldsymbol{R}_n) = \exp(\mathrm{i}\boldsymbol{k}\cdot\boldsymbol{R}_n)\psi_k(\boldsymbol{r}) \end{aligned} \tag{1}$$

or of the equivalent integral equation

$$\psi_k(\boldsymbol{r}) = \int_\Omega G_k(\boldsymbol{r}, \boldsymbol{r}'; E)V(\boldsymbol{r}')\psi_k(\boldsymbol{r}')\,\mathrm{d}^3\boldsymbol{r}'. \tag{2}$$

Here Ω is the unit-cell volume, $\{\boldsymbol{R}_n\}$ are the lattice translation vectors and the wavevector $\boldsymbol{k}$ lies within the first Brillouin zone. The Green function (GF), which meets the periodic boundary conditions, may be written as a series in the reciprocal lattice vectors $\boldsymbol{K}_\mu$:

$$G_k(\boldsymbol{r}, \boldsymbol{r}'; E) = -\frac{1}{\Omega}\sum_\mu \frac{\exp[\mathrm{i}(\boldsymbol{k}+\boldsymbol{K}_\mu)\cdot(\boldsymbol{r}-\boldsymbol{r}')]}{|\boldsymbol{k}+\boldsymbol{K}_\mu|^2 - E}. \tag{3}$$

A number of band-structure methods, such as Korringa–Kohn–Rostoker (KKR), augmented plane-wave (APW), linear muffin-tin orbitals (LMTO), and so on, are based on the well known 'muffin-tin' (MT) model for a crystal potential. Much effort has been made over the years to go beyond the MT model. The purpose is to develop a formalism,

delivering an exact solution to the problem (1) for a local crystal potential, which is a continuous function of point $\boldsymbol{r}$ except the nuclear positions. The principal difficulties are connected with the transformation from equation (2) to a set of algebraic equations in the angular momentum $|L\rangle \equiv |lm\rangle$ representation. The choice of this particular representation is caused by the essential feature of any crystal potential, which is close to a spherically symmetric function in local coordinates within a large enough portion of the unit cell.

The studies by Ziesche [1], Williams [2], Williams and van Morgan [3], Faulkner [4] and Brown and Ciftan [5] have outlined the ways in which the problem in question could be resolved. The aspiration to elaborate the theory as a straightforward extension of the multiple-scattering (MS) approach is revealed as a common feature of these works as well as many others [6–16]. Such an extension is based on the following interpretation of integral equation (2): an electron is scattered successively from one cell to another, and between the scattering events it is propagated as a free particle. This picture requires any crystal potential V be represented as a superposition of some individual cell potentials $v = v_n$, each of which vanishes beyond its 'own' cell Ω_n. Strictly speaking, a thin skin of thickness δ, adjoining the inner side of the cell surface, should be introduced. Because of the singular nature of the GF, each potential v_n must vanish within this skin too [17], and the final expressions should be obtained in the limit $\delta \to 0$.

In accordance with the essence of MS concept, one looks for the resulting wave field amplitude ψ_k (2) in the vicinity of cell surfaces. This approach is equivalent to matching both the fields ψ_k and $\nabla\psi_k$ across the cell boundaries. The corresponding techniques are based on two decisive assertions. First, the wavefunction ψ_k has to be expanded in a set of some basis functions, satisfying the Schrödinger equation with the individual cell potential v at an arbitrary energy E. Secondly, the GF should be expressed in the angular momentum representation [18] as

$$G_k(\boldsymbol{r}, \boldsymbol{r}'; E) = \kappa \sum_L j_L(\kappa, \boldsymbol{r}) n_L(\kappa, \boldsymbol{r}') + \sum_L \sum_{L'} B_{LL'}(\boldsymbol{k}, E) j_L(\kappa, \boldsymbol{r}) j_{L'}(\kappa, \boldsymbol{r}') \qquad r < r'. \tag{4}$$

Here $\kappa = \sqrt{E}$, and the abbreviated notations for some functions of 3D variable $\boldsymbol{r}$

$$j_L(\kappa, \boldsymbol{r}) \equiv j_l(\kappa r) Y_L(\hat{\boldsymbol{r}}) \qquad n_L(\kappa, \boldsymbol{r}) \equiv n_l(\kappa r) Y_L(\hat{\boldsymbol{r}}) \qquad \hat{\boldsymbol{r}} \equiv \boldsymbol{r}/r \tag{5}$$

are introduced. These functions are defined as products of real spherical harmonics Y_L and spherical Bessel j_l or Neumann n_l functions, respectively. For the sake of simplicity, we consider a crystal with only one atom per unit cell.

As a consequence of these assumptions, a set of homogeneous algebraic equations is obtained. The corresponding secular equation takes the form of generalised KKR one:

$$\det \left\| \kappa \cos \eta_{LL'}(\kappa) + \sum_{L''} B_{LL''}(\boldsymbol{k}, E) \sin \eta_{L''L'}(\kappa) \right\| = 0. \tag{6}$$

The generalised phase shifts $\eta_{LL'}(\kappa)$ describe the scattering of an electron with an energy $E = \kappa^2$ from the non-spherically symmetric potential v of the individual cell.

Ziesche was the first to recognise that equation (6) breaks down [1]. He was able to prove that, along the lines of the MS concept, a secular equation of factorised type (6), in which the quantities $\eta_{LL'}$ and $B_{LL'}$ would enter in a separate fashion, cannot be

derived. The simple expression (6) appears to be incorrect, because the GF expansion (4) is valid only if either

$$r < |r' + R_{\min}| \tag{7a}$$

or

$$r' < |r + R_{\min}| \tag{7b}$$

where $R_{\min}$ is the shortest among all the non-zero translations R_n. It appears that the double sum in expression (4) is only conditionally convergent, and the order of summations over L and L' depends upon specific positions of points r and r', by which either (7*a*) or (7*b*) are satisfied [5, 10]. According to the MS concept, the point r in equation (2) should run over the surface of the unit cell, and the point r' must run independently throughout the cell volume. Thus a uniformly and absolutely convergent GF expansion does not exist for such positions of points r and r'. Hence, when using this expansion (4) in equation (2), one cannot interchange the order of integration and summation, which is necessary to proceed to a set of algebraic equations.

A simple way to circumvent this obstacle is offered in our previous publication [19]. To achieve the above formulated goals, it is necessary to move away from treating the wave fields in the vicinity of cell boundaries. Instead, the amplitudes ψ_k should be sought at some points r belonging to spherical domain $\mathcal{D}$, centred at the cell origin. The radius of this domain $\mathcal{D}$ should be chosen in such a way that for each $r \in \mathcal{D}$ and each $r' \in \Omega$ the inequality $r + r' < R_{\min}$ be true. In such a case both the conditions (7) are satisfied simultaneously, and therefore the GF expansion (4) converges uniformly and absolutely. It is interesting to note that the possibility to handle the integral equation (2) at some arbitrary points r within a cell was already pointed out by Ziman [20]. Recently, the general formalism resulting from this *ansatz* has been presented [19]. Evidence has also been given [19] that in the specific case of a MT potential the general equations reduce to the well known KKR ones [17, 18].

The purpose of the present paper consists of the examination of this method by means of numerical treatment of the 3D Mathieu problem as well as of empty lattice tests. The main attention will be paid to studying the accuracy and the convergence properties.

In section 2 the method offered is outlined, and some parameters that govern the convergence are introduced explicitly. Section 3 contains the analytic solution of the 3D Mathieu problem. In section 4 the numerical aspects of practical calculations are considered. The computed results for empty lattice eigenvalues are discussed in section 5, and the ones for the 3D Mathieu problem are discussed in section 6. The paper is completed by the conclusions (section 7).

2. Outline of the method and convergence problem

Utilising both Green's theorem and the hermiticity of the Hamiltonian, one may transform equation (2) to a surface one:

$$\int_{\sigma} d\boldsymbol{\sigma}'[G_k(r, r'; E)\,\nabla'\psi_k(r') - \psi_k(r')\nabla' G_k(r, r'; E)] = 0 \qquad r \in \Omega. \tag{8}$$

Here $d\boldsymbol{\sigma}$ is the differential area element, directed along the outward normal to the surface σ of the cell Ω. To proceed from this integral equation (8) to a set of algebraic

equations, both the GF and wavefunction ψ_k should be expanded in some infinite series, which by a practical implementation are approximated by some finite sums. Thus a study of the convergence implies the determination of such numbers of terms in these sums, which provide a given accuracy. To make the convergence description easier, it is appropriate to turn to a symmetrised basis, by means of which some integer indices are naturally introduced. Thereby it is advisable to point out the numbers of terms in these sums explicitly.

Let the potential V of a one-atom crystal be invariant under the transformations of a point group $\mathcal{F}$, and let a vector $\boldsymbol{k}$ be invariant under the transformations of a group $\mathcal{F}_k$. Define a complete orthonormalised set of functions $\mathcal{K}_i^{\tau_k \nu}$, which are transformed according to the νth row of an irreducible representation τ_k of group $\mathcal{F}_k$, as some linear combinations of real spherical harmonics Y_L:

$$\mathcal{K}_i^{\tau_k \nu}(\hat{\boldsymbol{r}}) = \sum_m \alpha_{i,l_i m}^{\tau_k \nu} Y_{l_i m}(\hat{\boldsymbol{r}}). \tag{9}$$

The number i determines uniquely the value l_i of the corresponding angular momentum. (The indices $\tau_k \nu$ will be omitted everywhere except in statements allowing ambiguities.)

Consider the way in which the function ψ_k may be expanded. Let a cell Ω be circumscribed by a sphere $\mathbb{C}$. Define a set of some regular functions χ, which satisfy the Schrödinger equation at a given energy E and at all points $\boldsymbol{r} \in \mathbb{C}$:

$$[-\nabla^2 + V(\boldsymbol{r}) - E]\chi_{jE}^{\tau_k \nu}(\boldsymbol{r}) = 0 \qquad \boldsymbol{r} \in \mathbb{C}. \tag{10}$$

The regular solutions χ are set by the boundary conditions at $r = 0$ only, and their asymptotic behaviour at $r \to \infty$ is not subjected to any requirements. Their classification by numbers $j\tau_k \nu$ is governed by the transformation properties at $r \to 0$. These functions χ, defined within the circumscribed sphere $\mathbb{C}$, form a basis set, whose completeness and independence were proven by Brown and Ciftan ([5], equations (2.27) to (2.30)).

Each function ψ_k, satisfying equation (1), may be expanded in these basis functions χ_{jE} throughout the cell

$$\psi_k(\boldsymbol{r}) = \sum_{j=1}^{q} A_{jE}(\boldsymbol{k})\chi_{jE}(\boldsymbol{r}) \qquad \boldsymbol{r} \in \Omega, q \to \infty. \tag{11}$$

Within the circumscribed sphere both the potential V and the basis functions χ_{jE} may be expanded in symmetrised harmonics (9)

$$V(\boldsymbol{r}) = \sum_{i=1}^{p} v_i(r)\mathcal{K}_i^{\tau_1}(\hat{\boldsymbol{r}}) \qquad \boldsymbol{r} \in \mathbb{C}, p \to \infty \tag{12}$$

$$\chi_{jE}^{\tau_k \nu}(\boldsymbol{r}) = \frac{1}{r} \sum_{i=1}^{p} \varphi_{ij}^{\tau_k \nu}(r)\mathcal{K}_i^{\tau_k \nu}(\hat{\boldsymbol{r}}) \qquad \boldsymbol{r} \in \mathbb{C}, p \to \infty. \tag{13}$$

Here τ_1 is the identity representation of group $\mathcal{F}$. Define also a matrix with the elements

$$v_{iu}^{\tau_k \nu}(r) \equiv \iint \mathrm{d}\hat{\boldsymbol{r}} \mathcal{K}_i^{\tau_k \nu}(\hat{\boldsymbol{r}}) V(\boldsymbol{r}) \mathcal{K}_u^{\tau_k \nu}(\hat{\boldsymbol{r}}) \qquad \boldsymbol{r} \in \mathbb{C}. \tag{14}$$

Then the regular partial waves φ_{ij} satisfy the following set of Volterra integral equations [3]:

$$\varphi_{tj}(r) = \delta_{tj}\tilde{j}_{l_j}(\kappa r) + \frac{1}{\kappa}\int_0^r [\tilde{n}_{l_t}(\kappa r_>)\tilde{j}_{l_t}(\kappa r_<) - \tilde{j}_{l_t}(\kappa r_>)\tilde{n}_{l_t}(\kappa r_<)]$$
$$\times \sum_{u=1}^{p} v_{tu}(r')\varphi_{uj}(r')\,\mathrm{d}r' \tag{15}$$
$$r_< \equiv \min(r, r') \qquad r_> \equiv \max(r, r')$$
$$\tilde{j}_l(x) \equiv x j_l(x) \qquad \tilde{n}_l(x) \equiv x n_l(x).$$

Apparently the set (15) of size pq decomposes into q sets, each of which contains p bound equations. Namely, all the partial waves φ_{tj} $(t = 1, 2, \ldots, p)$ belong to one and the same set of a fixed number j. When solving this set, it is convenient to introduce so-called phase functions C and S [3, 5]:

$$\varphi_{tj}(r) = C_{tj}(r)\tilde{j}_{l_t}(\kappa r) + S_{tj}(r)\tilde{n}_{l_t}(\kappa r). \tag{16}$$

These phase functions satisfy in turn the following set of bound differential equations of first kind:

$$\frac{\mathrm{d}C_{tj}}{\mathrm{d}r} = -\frac{1}{\kappa}\tilde{n}_{l_t}(\kappa r)\sum_{u=1}^{p} v_{tu}(r)[\tilde{j}_{l_u}(\kappa r)C_{uj}(r) + \tilde{n}_{l_u}(\kappa r)S_{uj}(r)]$$
$$\frac{\mathrm{d}S_{tj}}{\mathrm{d}r} = \frac{1}{\kappa}\tilde{j}_{l_t}(\kappa r)\sum_{u=1}^{p} v_{tu}(r)[\tilde{j}_{l_u}(\kappa r)C_{uj}(r) + \tilde{n}_{l_u}(\kappa r)S_{uj}(r)] \tag{17a}$$

with the boundary conditions

$$C_{tj}(0) = \delta_{tj} \qquad S_{tj}(0) = 0. \tag{17b}$$

Also the GF expansion (4) must be rewritten as

$$G_k(\boldsymbol{r}, \boldsymbol{r}'; E) = \kappa \sum_{\tau k^\nu}\sum_{i=1}^{q} \mathcal{J}_i^{\tau k^\nu}(\kappa, \boldsymbol{r})\mathcal{N}_i^{\tau k^\nu}(\kappa, \boldsymbol{r}')$$
$$+ \sum_{\tau k^\nu}\sum_{i=1}^{q}\sum_{t=1}^{s} B_{it}^{\tau k^\nu}(\boldsymbol{k}, E)\mathcal{J}_i^{\tau k^\nu}(\kappa, \boldsymbol{r})\mathcal{J}_t^{\tau k^\nu}(\kappa, \boldsymbol{r}') \tag{18a}$$
$$r < r' \qquad r + r' < R_{\min} \qquad s \to \infty \qquad q \to \infty.$$

The symmetrised functions of 3D argument $\boldsymbol{r}$ (see (5))

$$\mathcal{J}_i^{\tau k^\nu}(\kappa, \boldsymbol{r}) \equiv j_{l_i}(\kappa r)\mathcal{H}_i^{\tau k^\nu}(\hat{\boldsymbol{r}}) \qquad \mathcal{N}_i^{\tau k^\nu}(\kappa, \boldsymbol{r}) \equiv n_{l_i}(\kappa r)\mathcal{H}_i^{\tau k^\nu}(\hat{\boldsymbol{r}}) \tag{18b}$$

and also the symmetrised structure constants

$$B_{it}^{\tau k^\nu} \equiv \sum_L \sum_{L'} \alpha_{iL}^{\tau k^\nu} B_{LL'} \alpha_{tL'}^{\tau k^\nu} \tag{18c}$$

are introduced here.

Now place a point $\boldsymbol{r}$ within such a spherical domain $\mathfrak{D}$, providing that for all $\boldsymbol{r} \in \mathfrak{D}$ and for all $\boldsymbol{r}' \in \Omega$ the condition $r + r' < R_{\min}$ holds true. Then substituting the expansions (11) and (18) into the integral equation (8), one may proceed to the desired set of

homogeneous algebraic equations with respect to some unknown coefficients A_{jE} [19]. The compatibility condition results in the following secular equation:

$$\det\left\| \kappa g_{ij}(\kappa) + \sum_{t=1}^{s} B_{it}(\boldsymbol{k}, E) f_{t_j}(\kappa) \right\| = 0 \qquad i = 1, 2, \ldots, q; j = 1, 2, \ldots, q. \tag{19}$$

Its zeros determine the eigenvalues sought. The quantities

$$\begin{aligned} f_{ij}(\kappa) &\equiv \oint \mathrm{d}\boldsymbol{\sigma}[\mathcal{J}_i(\kappa, \boldsymbol{r})\nabla\chi_{jE}(\boldsymbol{r}) - \chi_{jE}(\boldsymbol{r})\nabla\mathcal{J}_i(\kappa, \boldsymbol{r})] \\ g_{ij}(\kappa) &\equiv \oint \mathrm{d}\boldsymbol{\sigma}[\mathcal{N}_i(\kappa, \boldsymbol{r})\nabla\chi_{jE}(\boldsymbol{r}) - \chi_{jE}(\boldsymbol{r})\nabla\mathcal{N}_i(\kappa, \boldsymbol{r})] \end{aligned} \tag{20}$$

are defined as some integrals over the surface σ.

Some peculiarities of secular equation (19) are worth noting. It resembles the expression (6), obtained as a straightforward generalisation of the KKR MT equation [5, 9, 13]. However, the expressions, (6) and (19), are not identical. The distinction is caused by the various means in which the basis functions χ_{jE} are defined. In our case they are chosen as some solutions of equation (10) with the total potential V at each point $\boldsymbol{r} \in \mathbb{C}$. On the contrary, when obtaining the secular equation of type (6), some other functions are used. The latter satisfy equation (10) with the modified potential, which matches the original one at each point $\boldsymbol{r} \in \Omega$ and vanishes at $\boldsymbol{r} \notin \Omega$ [5]. So, the quantities f_{ij} and g_{ij} (20) are not proportional to sin η_{ij} and cos η_{ij}, respectively. Incidentally, this abrupt truncation of the potential v at the surface of the cell, forced by MS requirements, results in a worse convergence of multipole decomposition (12).

By a practical realisation the secular equation (19) determines an approximate energy eigenvalue, numbered by three independent parameters p, q and s, arising as a consequence of truncating the infinite series (13), (11) and (18), respectively. The number of basis functions χ included in the expansion (11) determines the size q of secular matrix (19). The number of components retained in GF expansion (18) determines the number s of terms that contribute to each matrix element (19). And finally, the number p of partial waves φ_{ij} $(t = 1, 2, \ldots, p)$ included in expansion (13) of basis function χ_{jE} affects the value of each integral f or g (20). Hence, before studying the convergence of eigenvalues against the size q of secular matrix, the convergence of each matrix element (19) against s should be ensured, and the same holds for the convergence of each integral f_{ij} or g_{ij} (20) against the number p. In such a general treatment, the description of convergence properties will be very involved. To simplify the investigation we have arbitrarily set $p = s$ (except for MT and empty lattice cases; see below). The corresponding estimate for an energy eigenvalue we shall denote as $E_{q/s}$.

This manner of convergence differs substantially from the one in MT approximation. It is easy to show that $p = 1$ in the MT case, and additionally the off-diagonal integrals f_{ij}^{MT} and g_{ij}^{MT} $(i \neq j)$ do vanish [19]. From equation (19) it follows that in the MT model the convergence depends upon a single parameter q (the size of the secular matrix), which is conventionally described by a value $l_{\max} = l_q$ of the principal angular momentum.

3. Three-dimensional Mathieu potential: analytical solution

It is pertinent to perform numerical studies of the method considered by means of a model, the exact solutions of which are known. Such a possibility is afforded by the

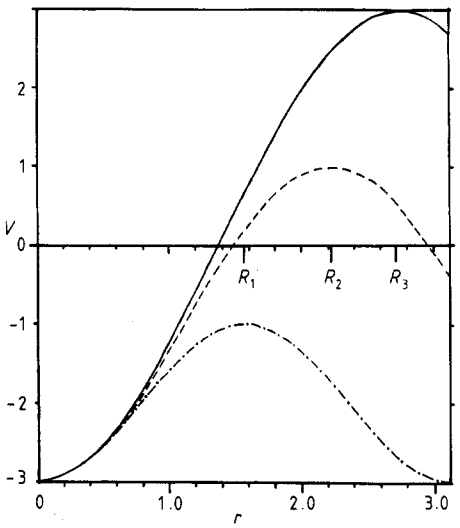

Figure 1. The radial dependence of the 3D Mathieu potential (21) with $U_1 = 0$ and $U_2 = -1$ along the three directions in a simple cubic cell: —— [111], ---- [011], —·—·— [001]; $R_1 = \frac{1}{2}\pi$, $R_2 = \frac{1}{2}\pi\sqrt{2}$, $R_3 = \frac{1}{2}\pi\sqrt{3}$.

periodic solutions of the 3D Mathieu problem. Consider a potential

$$V(r) = U_1 + U_2[\cos(2\pi x/a) + \cos(2\pi y/a) + \cos(2\pi z/a)] \tag{21}$$

by means of which a simple cubic (SC) lattice is brought into consideration. U_1 and U_2 are free parameters. Define a dimensionless energy $\varepsilon = (a/2\pi)^2 E$, and let $a = \pi$. The 3D equation (1) with the potential (21) may be decomposed into three ordinary differential equations. Hence the energy eigenvalues of the initial 3D problem may be found, provided the eigenvalues d of the so-called canonical Mathieu equation [21]

$$d^2y/dx^2 + (d - U_2 \cos 2x)\, y = 0 \tag{22}$$

are known. In particular, the eigenvalues $\bar{\varepsilon}$ of the 3D problem at the point Γ ($\boldsymbol{k} = 0$) are expressed by means of eigenvalues a_{2r} and b_{2r} ($r = 0, 1, \ldots$), corresponding to even and odd periodic solutions of equation (22), respectively. In specific cases of lowest levels with symmetries Γ_1, Γ_{15} and Γ_{12}, in a SC lattice the following expressions result:

$$\begin{aligned} \bar{\varepsilon}_{1\Gamma_1} &= \tfrac{1}{4}(U_1 + a_0 + a_0 + a_0) & \bar{\varepsilon}_{1\Gamma_{15}} &= \tfrac{1}{4}(U_1 + a_0 + a_0 + b_2) \\ \bar{\varepsilon}_{1\Gamma_{12}} &= \tfrac{1}{4}(U_1 + a_0 + a_0 + a_2) & \bar{\varepsilon}_{2\Gamma_{15}} &= \tfrac{1}{4}(U_1 + a_0 + a_2 + b_2). \end{aligned} \tag{23}$$

The method offered (see section 2) may also be applied to the 3D Mathieu problem. For this purpose it is necessary to find the components $v_i(r)$ (12) of the potential (21). The first five symmetrised components are presented below:

$$\begin{aligned} v_1(r) &= 2\pi^{1/2}[U_1 + 3U_2 j_0(2r)] \\ v_2(r) &= 24.36720 \times U_2 j_4(2r) & v_3(r) &= -13.55665 \times U_2 j_6(2r) \\ v_4(r) &= 31.48599 \times U_2 j_8(2r) & v_5(r) &= -19.97225 \times U_2 j_{10}(2r). \end{aligned}$$

These expressions give evidence that, by increasing the number i, the components $v_i(r)$ approach zero sufficiently rapidly in the whole range $0 \leqslant r \leqslant \frac{1}{2}\pi\sqrt{3}$ of radial variable r.

Note that the 3D Mathieu potential (21) is represented by a highly anisotropic function. The degree of anisotropy may be displayed by plotting the potential along the three directions in a cubic cell (figure 1). The potential is close to a spherically symmetric

function over a small enough portion of cell volume ($r \lesssim 0.5$). The magnitude of the variations of the potential with the angles at the radius of the inscribed sphere ($r = \frac{1}{2}\pi$) reaches a value $\simeq 1.5$, while the total potential within the cubic cell varies from the value -3.0 in the centre to $+3.0$ at the corners. Such a strong anisotropy of 3D Mathieu potential permits one to consider it as a good test for methods pretending to exact solution.

4. Numerical aspects of the calculations

The rate of convergence of the expansion (13) is obviously dependent upon the degree of crystal potential anisotropy. If the potential could be a spherically symmetric function (it is clearly impossible for any crystal), that is, if $v_{ij}(r) = 0$ for $t \neq j$, then all the off-diagonal waves $\varphi_{ij}(r)$ $(t \neq j)$ do vanish. Therefore, the single partial wave φ_{jj} might contribute to the basis function χ_{jE}. The higher the degree of anisotropy, the more terms should be included in the expansion (13). The number p of these terms determines the size $2p$ of the set (17) of bound differential equations of first order. To find the phase functions C and S, satisfying the set (17), we use the Runge–Kutta method.

Once the basis functions χ_{jE} as sums (13) have been computed, one may proceed to the estimation of integrals f_{ij} and g_{ij} (20). Substantial simplifications are reached if, by computation of gradients of 3D functions entering the integrands in expressions (20), the numerical methods are eliminated. Keeping this in mind, we represent these integrands as some sums of products of functions depending upon radial variable only and functions depending upon angular variables only (see (13) and (18*b*)). The gradients of angle-dependent parts are computed analytically by means of symbolic programming system REDUCE [22]. Hence numerical methods are required only for the computations of values of partial waves φ_{ij} and of their radial derivatives at an arbitrary point on the cell surface. To this end we apply a spline interpolation routine.

The symmetry of integrands in expressions (20) allows us to reduce the integration to the irreducible part of the cell surface (1/48th part in the case of cubic symmetry). Until the number j is not large enough, the integrands (20) exhibit a few oscillations within the irreducible part. Therefore, for this surface integration it is appropriate to use some standard methods such as the Simpson routine. The accuracy of the calculations may be checked by test examples—MT model and zero potential—which both allow the analytic computations of integrals (20).

The structure constants B_{ij} (18*a*) have been computed by means of the Ewald technique [18].

We do not quote here the accuracy with which these intermediate functions and quantities mentioned above (φ, χ, $\mathbf{f}$, $\mathbf{g}$, $\mathbf{B}$) are computed, because that information requires too much space, and it may be the subject of a separate publication. Instead, we prefer to consider the accuracy of the resulting eigenvalues, reflecting all the individual accuracies in a cumulative fashion.

5. Empty lattice test

The dimensionless eigenvalues $\bar{\varepsilon}$ of an empty SC lattice with constant potential $V(r) = U_1$ may be obtained as singularities of the GF (3):

$$\bar{\varepsilon} = \tfrac{1}{4}[U_1 + |\boldsymbol{k} + \boldsymbol{K}_\mu|^2].$$

Consider the point Γ $(\boldsymbol{k} = 0)$. The lowest level $1\Gamma_1$ with the energy $\bar{\varepsilon} = \frac{1}{4}U_1$ is non-

Table 1. Calculated $\varepsilon_{1/s}$ and exact $\bar{\varepsilon}$ energy eigenvalues $1\Gamma_1$ for empty simple cubic lattice ($a = \pi$).

U_1	$\varepsilon_{1/1}$	$\varepsilon_{1/2}$	$\varepsilon_{1/3}$	$\varepsilon_{1/4}$	$\varepsilon_{1/5}$	$\bar{\varepsilon}$
−0.4	−0.1021	−0.0995	−0.0998	−0.1001	−0.1000	−0.1
−0.8	−0.2085	−0.1985	−0.1994	−0.2003	−0.2000	−0.2
−1.2	−0.3195	−0.2960	−0.2985	−0.3009	−0.3000	−0.3
−1.6	−0.4355	−0.3925	−0.3973	−0.4016	−0.4000	−0.4
−2.0	−0.5577	−0.4880	−0.4956	−0.5029	−0.5000	−0.5

degenerate. The six-fold degenerate level $\bar{\varepsilon} = \frac{1}{4}U_1 + 1$ corresponds to the set $\{1\,0\,0\}$ of reciprocal lattice vectors, forming the states $1\Gamma_{15}$, $1\Gamma_{12}$ and $2\Gamma_1$. The 12-fold degenerate level $\bar{\varepsilon} = \frac{1}{4}U_1 + 2$ corresponds to the vectors $\{1\,1\,0\}$, forming the states $3\Gamma_1$, $2\Gamma_{12}$, $2\Gamma_{15}$, $1\Gamma_{2'5}$ and $1\Gamma_{25}$. The corresponding eigenstates occur as some symmetrised combinations of plane wave $\exp(i\boldsymbol{K}_\mu \cdot \boldsymbol{r})$.

Now turn to the discussion of numerical results. In the case of constant potential U_1, all the off-diagonal matrix elements (14) vanish, and $v_{ii}(r) = U_1$ for each value i. Consequently, the set (15) of bound equations breaks into independent ones, and the sole partial wave

$$\varphi_{jj}(r) \sim \tilde{j}_{l_j}((E - U_1)^{1/2} r) \tag{24}$$

contributes to the corresponding basis function χ_{jE} (13). It means that in the empty lattice test the number p is equal to 1.

The band bottom $1\Gamma_1$ ($E = U_1$) represents a particular case. Indeed, its true wavefunction is equal to a constant. Hence it follows that only one basis function $\chi_1^{\Gamma 1}$, which corresponds to angular momentum $l = 0$, may contribute to the expansion (11), because all the remaining functions (24) with $j \neq 1$ tend to zero as E approaches U_1. Therefore a non-trivial solution is obtained if the size q of secular matrix is equal to 1. Thus, the energy eigenvalue $1\Gamma_1$ may be obtained merely as a zero of the following equation:

$$\kappa g_{11}(\kappa) + \sum_{n=1}^{s} B_{1n}(0, E) f_{n1}(\kappa) = 0 \qquad s \to \infty. \tag{25}$$

Thus, an estimate of the eigenvalue $1\Gamma_1$ depends on the single parameter s. The convergence of the calculated eigenvalues $\varepsilon_{1/s}$ to exact ones $\bar{\varepsilon}$ is displayed in table 1. For each given s the absolute value of deviation (AVD) $|\Delta\varepsilon| = |\varepsilon_{1/s} - \bar{\varepsilon}|$ increases if $|U_1|$ rises. At the same time, for each given value U_1 the calculated AVD $|\Delta\varepsilon|$ approach zero if the number s increases. In particular, for each $|U_1| \leqslant 2.0$, AVD $|\Delta\varepsilon_{1/5}|$ are less than 0.0001. It is advisable to list the angular momentum values in the representation Γ_1: $l_1 = 0$, $l_2 = 4$, $l_3 = 6$, $l_4 = 8$, $l_5 = 10$.

The convergence of all other empty lattice states is governed by two independent parameters q and s. As an example, let us consider the deviations $\Delta\varepsilon_{q/s} = \varepsilon_{q/s} - \bar{\varepsilon}$ for the state $2\Gamma_{15}$, displayed as functions of number s ($s = 1, 2, \ldots, 12$) at some fixed values q ($q = 1, 2, \ldots, 6$) in figure 2. (The cubic harmonics $\mathcal{H}_i^{\Gamma 15 1}$ (9) match precisely the real spherical harmonics $Y_{l_i m_i}$, and thus the functions $\{l_i m_i\} = \{1,0; 3,0; 5,0; 5,4; 7,0; 7,4; 9,0; 9,4; 9,8; 11,0; 11,4; 11,8\}$ contribute to this set of 12 functions.) The zeros of determinants of first, second and third orders converge rapidly against s at all values U_1 studied: when $s \geqslant 6$, AVD $|\Delta\varepsilon|$ are smaller than 0.0001. The converged values $\varepsilon_{q/12} \simeq$

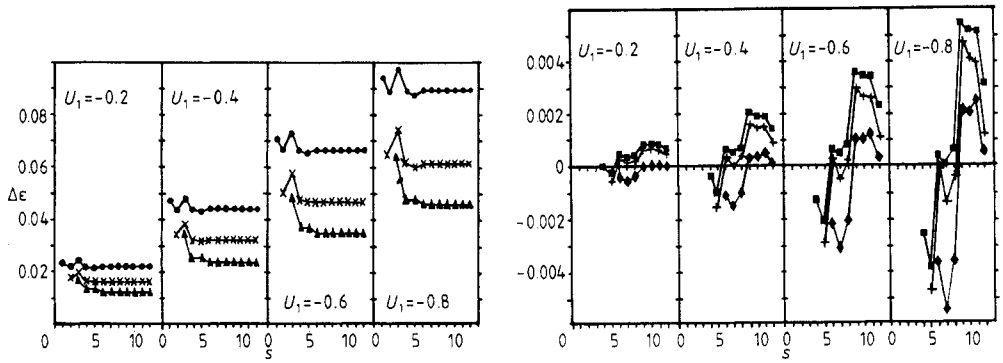

Figure 2. The deviations $\Delta\varepsilon_{q/s} = \varepsilon_{q/s} - \bar{\varepsilon}$ of the calculated energy eigenvalues $\varepsilon_{q/s}$ from the exact ones $\bar{\varepsilon}$ for the state $2\Gamma_{15}$ of a simple cubic lattice ($a = \pi$). Note the different scales in the left hand side ($q \leqslant 3$) and in the right hand side ($q \geqslant 4$) of the figure —●—●— $q = 1$; —×—×— $q = 2$; —▲—▲— $q = 3$; —■—■— $q = 4$; —+—+— $q = 5$; —◆—◆— $q = 6$.

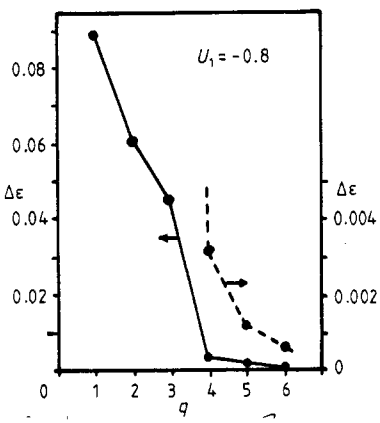

Figure 3. The deviations $\Delta\varepsilon_{q/12}$ for the state $2\Gamma_{15}$ of an empty simple cubic lattice versus the order q of the secular matrix.

$\varepsilon_{q/\infty}$ differ from the corresponding exact ones $\bar{\varepsilon}$ by quantities of the order 0.01 to 0.1 (see the left part of figure 2). When $q \geqslant 4$, the energies $\varepsilon_{q/s}$ oscillate around the exact values (see the right part of figure 2). If $|U_1|$ increases, the magnitude of these oscillations grows. When $U_1 = -0.2$, the energies $\varepsilon_{4/s}$, $\varepsilon_{5/s}$ and $\varepsilon_{6/s}$ converge quickly against s. Note that the converged value of sixth-order matrix practically matches the exact one (when $s \geqslant 9$, $|\Delta\varepsilon_{6/s}| < 0.0001$). When $U_1 = -0.8$, for reliable observation of convergence, values of s larger than 12 are evidently needed.

The conventional investigation of convergence implies the study of an eigenvalue against the size q of corresponding secular matrix. In figure 3 the difference $\Delta\varepsilon_{q/12} = \varepsilon_{q/12} - \bar{\varepsilon}$ as a function of size q is presented. Dependences of such a kind are comprehensive only if the respective eigenvalues prove to be converged against s ($\varepsilon_{q/12} \simeq \varepsilon_{q/\infty}$). Nevertheless, one can see that the deviations $\Delta\varepsilon_{q/12}$ tend to zero monotonically from above. In particular, when $U_1 = -0.8$, the difference $\Delta\varepsilon_{6/12}$ is equal to 0.0006.

Similar trends are also observed in the behaviour of eigenvalues $1\Gamma_{15}$ and $1\Gamma_{12}$. Summarising, one may conclude that, when the parameters s and q are increased, the calculated energy eigenvalues $\varepsilon_{q/s}$ tend to match the exact ones $\bar{\varepsilon}$. The larger the

Table 2. The deviations $\Delta\varepsilon_{q/s}$ of calculated eigenvalues $\varepsilon_{q/s}$ from the exact ones $\bar{\varepsilon}$ for $2\Gamma_{15}$ state of the 3D Mathieu potential (21) ($U_1 = -0.2$, $U_2 = -0.1$, $a = \pi$).

	$\Delta\varepsilon_{q/s} \times 10^4$											
q	$s=1$	$s=2$	$s=3$	$s=4$	$s=5$	$s=6$	$s=7$	$s=8$	$s=9$	$s=10$	$s=11$	$s=12$
1	72	72	85	95	92	92	92	92	92	92	92	92
2	–	25	34	49	51	46	47	47	47	47	47	47
3	–	–	10	31	27	21	27	27	26	26	27	27
4	–	–	–	−11	−14	−18	−12	−9	4	4	5	5

magnitude U_1, the more terms s should be accounted for in each element of the secular matrix, and the larger the values q of its size should be taken, if a given accuracy is required to be reached. Comparison of various levels shows that the rate of convergence is mainly governed by the corresponding energies: the higher a level, the slower is convergence. For instance, the levels $2\Gamma_1$ and $3\Gamma_1$ converge slower than level $1\Gamma_1$.

The empty lattice test was also studied by means of methods that represent the direct extension of the MS approach. Both the 3D case [3, 13, 23–25] and the 2D case [11, 14] were considered. From most of these investigations it follows that, similar to the MT model, the convergence is governed by the single parameter $l_{\max}$. According to our analysis, this mode of investigation may be reproduced by setting arbitrarily $q = s$. However, our numerical experience shows that this degree of approximation appears to be insufficient, and values $s \geqslant q$ are generally required. This phenomenon is clearly seen in the case of the $1\Gamma_1$ state (table 1).

As a result of 2D calculations for an empty square lattice, it was previously noted that the convergence rate of an excited state with a fixed symmetry, e.g. $2\Gamma_0$, is slower than for a lowest state with some different symmetry, e.g. $1\Gamma_2$ [14]. Zeller [11] regarded this as a consequence of the special form of secular matrix used by Faulkner [14], by which the inverse of the nearly degenerate t matrix should be computed. This difficulty is not inherent to the secular matrix (19) used in our calculations.

6. Three-dimensional Mathieu problem: results of calculations

Consider now the calculated energy eigenvalues of the 3D Mathieu problem. The exact eigenvalues $\bar{\varepsilon}$ are defined by means of expressions (23). For the specific case of $2\Gamma_{15}$ state the deviations $\Delta\varepsilon_{q/s} = \varepsilon_{q/s} - \bar{\varepsilon}$ are displayed in table 2. One can see that the zeros of first and second orders converge rapidly enough against s: when $s \geqslant 6$, the variations of the deviations $\Delta\varepsilon_{1/s}$ and $\Delta\varepsilon_{2/s}$ do not exceed 0.0001. As to the zeros of third and fourth orders, for more reliable fixation of the converged energies with the chosen accuracy of 0.0001 somewhat larger values of parameter s are desired. If the required degree of convergence against s is reached (that is, if $\varepsilon_{q/12}$ may serve as $\varepsilon_{q/\infty}$), then the dependences of values $\varepsilon_{q/12}$ upon q are sensible. When q increases, the deviations $\Delta\varepsilon_{q/12}$ approach zero monotonically from above (see the last column of table 2). Thus even for a level with such a high energy ($\bar{\varepsilon}_{2\Gamma_{15}} = 1.9499$) to reach the accuracy of 0.0005, it is sufficient to calculate zeros of fourth-order determinant ($l_4 = 5$) with $s = 12$ ($l_{12} = 11$).

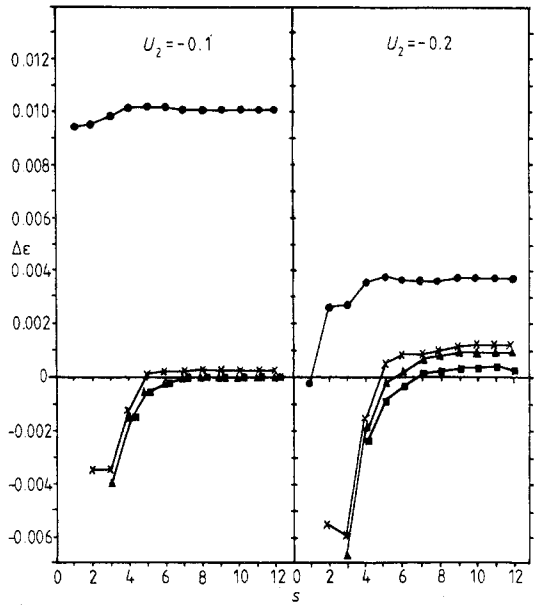

Figure 4. The deviations $\Delta\varepsilon_{q/s}$ for the state $1\Gamma_{15}$ of the 3D Mathieu problem (21) with $U_1 = -0.2$, $U_2 = -0.1$ (left), and $U_1 = -0.2$, $U_2 = -0.2$ (right): —●—● $q = 1$; —×—×— $q = 2$; —▲—▲— $q = 3$; —■—■— $q = 4$.

Similar results are obtained by studying the states $1\Gamma_{15}$, $1\Gamma_1$ and $1\Gamma_{12}$. In figure 4 as an additional example the deviations $\Delta\varepsilon_{q/s}$ for the state $1\Gamma_{15}$ are displayed. The main trends are the same as for $2\Gamma_{15}$, though the convergence of $1\Gamma_{15}$ eigenvalue is more rapid. This phenomenon is obviously connected with the difference in their absolute energies. In particular, when $U_2 = -0.1$, the AVD $|\Delta\varepsilon_{4/12}|$ is less than 0.0001. If $|U_2|$ increases, the AVD $|\Delta\varepsilon_{q/s}|$ also grow. To reach a given accuracy, both the size q of secular matrix and the number s of terms contributing to each matrix element should be increased, if larger values $|U_2|$ are used.

Nevertheless, numerical experience for a sufficiently wide range of values U_2, performed for some fixed values q and s, has demonstrated that the deviation $\Delta\varepsilon_{q/s}$ appears to be an oscillating function of U_2 rather than monotonic. Thus by means of some fixed values q and s one may obtain approximate (non-converged) estimations of eigenvalues. The energies evaluated in this manner for the states $1\Gamma_1$, $1\Gamma_{15}$ and $1\Gamma_{12}$ over a wide range of the parameter U_2 are compared with the exact ones in table 3. Some preliminary results obtained with smaller values of parameter s, were presented in [19].

When for the state $1\Gamma_1$ the approximation '3/7' is chosen, the maximum AVD $|\Delta\varepsilon|$ does not exceed 0.003. Similarly in the case $1\Gamma_{15}$ the approximation '4/6' allows one to reach an accuracy of $\simeq$0.002, and in the state $1\Gamma_{12}$ for the approximation '3/9' the AVD are less than 0.004.

7. Conclusions

A thorough investigation of the method [19] assigned to solve the non-MT band-structure problem exactly shows that an approximate energy eigenvalue is determined by three independent parameters, which are connected with the truncations of series for GF, basis functions and wavefunction. In the case of a MT potential the degree of approximation is governed by a single parameter l_{max}. The numerical results obtained for some empty

Table 3. The calculated eigenvalues $\varepsilon_{q/s}$ and the exact ones $\bar{\varepsilon}$ (23) for the 3D Mathieu potential versus U_2 ($U_1 = -0.4$, $a = \pi$).

	$1\Gamma_1$		$1\Gamma_{15}$		$1\Gamma_{12}$	
U_2	$\varepsilon_{3/7}$	$\bar{\varepsilon}$	$\varepsilon_{4/6}$	$\bar{\varepsilon}$	$\varepsilon_{3/9}$	$\bar{\varepsilon}$
−0.4	−0.1145	−0.1149	0.8889	0.8892	0.8944	0.8942
−0.8	−0.1578	−0.1590	0.8577	0.8573	0.8776	0.8770
−1.2	−0.2292	−0.2301	0.8069	0.8058	0.8492	0.8491
−1.6	−0.3227	−0.3253	0.7382	0.7365	0.8104	0.8115
−2.0	–	–	0.6539	0.6517	0.7629	0.7653
−2.4	–	–	0.5558	0.5535	0.7085	0.7114
−2.8	–	–	0.4459	0.4438	0.6487	0.6508
−3.2	–	–	0.3259	0.3243	0.5846	0.5844
−3.6	–	–	0.1974	0.1963	0.5169	0.5127

lattice and 3D Mathieu tests show that by increasing all three parameters mentioned the calculated energy eigenvalues approach the exact ones.

As far as we know, the numerical solution of the 3D Mathieu problem has been attempted in the present study for the first time. (Moreover, in a recently published paper, it was declared that the 'empty lattice model is the only 3D model of a non-MT potential that I am aware of for which the exact eigenvalues are known' [23].) The previous investigations, performed by means of generalised MS approaches, are restricted to some empty lattice tests only, including 3D [3, 13, 23–25] as well as 2D [11, 14] cases. Unfortunately, we cannot compare our empty lattice results with the cited ones for two reasons. First, all the studies referred to are related to a body-centred cubic (BCC) lattice, rather than a SC one. Secondly, the mentioned 3D results are displayed by means of RMS deviations of calculated eigenvalues for a number of states, which form a degenerate level. On the contrary, we have studied the deviations for each individual state. The SC lattice was chosen because it represents a more crucial test: the shapes of BCC or FCC cells are closer to a sphere, so in a SC lattice the effects of anisotropy should be more pronounced.

Additionally, the anisotropy of the 3D Mathieu potential in a SC lattice exceeds essentially any conceivable anisotropy of a potential that describes an arbitrary many-atom system. Therefore successful computations for the 3D Mathieu potential in a SC lattice allow one to expect that the method offered will serve as a useful tool in electronic structure theory.

References

[1] Ziesche P 1974 *J. Phys. C: Solid State Phys.* **7** 1085–97
[2] Williams A R 1974 *Int. J. Quantum Chem. Symp.* **8** 89–108
[3] Williams A R and van Morgan J W 1974 *J. Phys. C: Solid State Phys.* **7** 37–60
[4] Faulkner J S 1979 *Phys. Rev.* B **12** 6186–206
[5] Brown R G and Ciftan M 1983 *Phys. Rev.* B **27** 4564–79
[6] Gonis A 1986 *Phys. Rev.* B **33** 5914–16
[7] Gonis A, Zhang X-G and Nicholson D M 1988 *Phys. Rev.* B **38** 3564–7
[8] Zhang X-G and Gonis A 1989 *Phys. Rev.* B **39** 10373–5
[9] Gonis A, Zhang X-G and Nicholson D M 1989 *Phys. Rev.* B **40** 947–65

[10] Zeller R 1987 *J. Phys. C: Solid State Phys.* **20** 2347–60
[11] Zeller R 1988 *Phys. Rev.* B **38** 5993–6002
[12] Molenaar J 1988 *J. Phys. C: Solid State Phys.* **21** 1455–68
[13] Faulkner J S 1986 *Phys. Rev.* B **34** 5931–4
[14] Faulkner J S 1988 *Phys. Rev.* B **38** 1686–94
[15] Badralexe E and Freeman A J 1987 *Phys. Rev.* B **36** 1378–88; 1988 *Phys. Rev.* B **37** 1067–84, 10469–74
[16] Brown R G and Ciftan M 1989 *Phys. Rev.* B **39** 3543–50
[17] Kohn W and Rostoker N 1954 *Phys. Rev.* **94** 1111–20
[18] Ham F S and Segall B 1961 *Phys. Rev.* **124** 1786–96
[19] Gegusin I I and Leontieva L I 1989 *Sov. Phys.-JETP* **96** 1075–86
[20] Ziman J M 1971 *Solid State Physics* vol 26, ed H Ehrenreich, F Seitz and D Turnbull (New York: Academic) p 77
[21] Abramowitz M and Stegun I A 1964 *Handbook of Mathematical Functions* (Washington DC: National Bureau of Standards)
[22] Hearn A C 1983 *REDUCE User's Manual* Rand Corporation Publ. CP78(4/83) (Santa Monica: Rand)
[23] Faulkner J S 1985 *Phys. Rev.* B **32** 1339–42
[24] Brown R G and Ciftan M 1985 *Phys. Rev.* B **32** 1343–6
[25] Brown R G and Ciftan M 1986 *Phys. Rev.* B **33** 7937–40